Influence of Product Phase Separation on Phospholipase A_2 Hydrolysis of Supported Phospholipid Bilayers Studied by Force Microscopy

Lars K. Nielsen,*† Konstatin Balashev,† Thomas H. Callisen,* and Thomas Bjørnholm†
*Department of Chemistry, Technical University of Denmark, DK-2800 Lyngby, and †Nano-Science Center, Department of Chemistry, University of Copenhagen, DK-2100 Copenhagen, Denmark

ABSTRACT In situ atomic force microscopy studies reveal a marked influence of the initial presence of hydrolysis products on the hydrolysis of supported phospholipid bilayers by phospholipase A_2. By analysis of the nano-scale topography of a number of supported bilayers with different initial product concentrations, made by Langmuir-Blodgett deposition, we show that small depressions enriched in products are efficiently promoting enzyme degradation of the bilayer. These small depressions, which are indicative of phase separation, are initially present in samples with 75% products. The kinetics of phospholipase A_2 exhibit under certain conditions an initial phase of slow hydrolysis, termed the latency phase, followed by a marked increase in the hydrolysis rate. The appearance of the phase-separated bilayer is strikingly similar to that of bilayers at the end of the latency phase. By analysis of individual nano-scale defects we illustrate a quantitative difference in the growth rates of defects caused by product aggregation and other structural defects. This difference shows for the first time how the enzyme prefers one type of defect to another.

INTRODUCTION

The hydrolysis of phospholipids at the *sn*-2 position by phospholipase A_2 (PLA_2) is for lipid bilayer membranes characterized by a latency period, i.e., a period of low activity, followed by a burst in activity (Apitz-Castro et al., 1982). The burst has been suggested to be caused by the accumulation of hydrolysis products, free fatty acid and 1-acyl-lyso-phospholipid, created during the latency period, which alter the susceptibility of the phospholipid membranes to degradation by the phospholipase (Apitz-Castro et al., 1982; Burack et al., 1993; Henshaw et al., 1998). The reaction is biologically important as PLA_2 plays a role in many physiological processes such as lipid metabolism, inflammation, and signaling (Waite, 1991; Kudo et al., 1993; Mayer and Marshall, 1993; Vadas et al., 1993). The course of the reaction is to a large extent determined by the properties of the membrane with which the PLA_2 interacts. Special attention has been given to the duration of the latency period, which can be modulated by varying the experimentally accessible parameters such as Ca^{2+} concentration, ionic strength, temperature, lipid composition, density fluctuations, vesicle curvature, and addition of hydrolysis products (Fernández et al., 1991; Ghomashchi et al., 1991; Muderhwa and Brockman, 1992; Hønger et al., 1996; Nielsen et al., 2000). The changes induced by the addition of products and the role of the products during the different stages of hydrolysis have received great attention (Brown et al., 1993; Burack et al., 1993, 1997a; Burack and Biltonen, 1994; Hønger et al., 1997; Callisen and Talmon, 1998; Henshaw et al., 1998; Wilson et al., 1999). For large unilamellar vesicles of dipalmitoylphosphatidylcholine (DPPC), the product concentration that abolishes the lag phase have been reported to lie close to 8 mol % (Burack and Biltonen, 1994). Thermodynamic data indicate that phase separation also occurs at a product concentration of 8 mol % (Burack et al., 1993, 1997a). The individual roles of the hydrolysis products have been determined by Henshaw et al. (1998). They showed that ionized fatty acids promoted calcium-independent binding of the phospholipase to vesicles through electrostatic interaction. Lyso-lipid enhanced the membrane susceptibility to the enzyme attack but at the same time attenuated the binding of PLA_2 by changing the structure of the fatty acid domains (Henshaw et al., 1998). In addition to phase separation, increasing amounts of hydrolysis products also lead to vast morphological changes in vesicular systems (Burack et al., 1997b; Callisen and Talmon, 1998). The original vesicular suspension changes into a poorly defined mixture of punctured vesicle, disk micelles, and normal micelles. Recent structural studies by cryo-transmission electron microscopy have shown that these changes take place already during the latency period where only a few percent of the substrate molecules have been hydrolyzed. In this case, a cascade process where the initial changes in lipid composition alter the morphology of the substrate, which in turn enhances the rate of hydrolysis, has been suggested (Callisen and Talmon, 1998).

High-resolution structural techniques such as atomic force microscopy (AFM) and x-ray scattering have been used in the characterization of the interaction between lipases and its substrate (Grandbois et al., 1998; Beisson et al., 2000; Balashev et al., 2001; Jensen et al., 2001). We recently reported the presence of a latency period in supported phospholipid bilayers (Nielsen et al., 1999). Our

Submitted November 12, 2001, and accepted for publication June 14, 2002.

T. H. Callisen's present address: Novo Nordisk A/S, Novo Allé, 2880 Bagsværd, Denmark.

Address reprint requests to Dr. Thomas Bjørnholm, Department of Chemistry, University of Copenhagen, Universitetsparken 5, DK-2100 Copenhagen, Denmark. Tel.: 45-35321835; Fax: 45-35321810; E-mail: tb@nano.ku.dk.

0006-3495/02/11/2617/08 $2.00

combined kinetic and structural study of the hydrolysis of supported DPPC bilayers by AFM revealed small depressions formed during the latency period indicative of domain formation by the products created in the early stages of hydrolysis. The data furthermore showed that the burst in activity was centered around the product domains and the disruption of the lipid bilayer started at these depressions. The advantage of using supported bilayers as a substrate for PLA_2 hydrolysis is that they are morphologically well defined structures and one can increase the product concentration range and eliminate shape and curvature changes from the interpretation.

In the present study, we have exploited this advantage by varying the initial product concentration in supported phospholipid bilayers. The accessible product concentration range was 0–100% with the same initial morphology for all concentrations. This range exceeds the accessible range when using vesicular substrates by far.

MATERIALS AND METHODS

Langmuir-Blodgett films

Monolayers with initial product concentrations from 0% to 100% were prepared on a commercial Langmuir trough (KSV 5000, KSV, Helsinki, Finland). Freshly cleaved mica was used as the solid support, which was immersed in the subphase before the spreading of the phospholipids and palmitic acid. 1,2-Dipalmitoyl-*sn*-glycero-3-phosphocholine (DPPC), palmitic acid (PA), and 1-palmitoyl-2-hydroxy-*sn*-phosphocholine (lyso-PPC) (Avanti Polar Lipids, Alabaster, AL) was dissolved in *n*-hexane: methanol (95:5) to a concentration between 0.6 and 1 mg/ml. The spreading from a hexane solution is much less vigorous and improves reproducibility of the isotherms compared with spreading from a chloroform solution. From the stock solutions mixtures with the desired product concentration were produced. The lipids were spread on a pure MilliQ (Millipore Corp., Bedford, MA) water surface, and 15–30 min was allowed for solvent evaporation. The monolayers were compressed at a constant speed of 1 $Å^2$/molecule/min to a final surface pressure in the liquid-condensed phase of typically 30–35 mN/m. We have obtained isotherms for each of the components DPPC, lyso-PPC, and PA individually and of their mixtures, which are similar to those previously reported (Maloney and Grainger, 1993). In the mixed systems, the ratio between lyso-PPC and PA is always 1:1. These mixed systems nominally correspond to different degrees of hydrolysis. All the substances form stable monolayers that can be transferred to solid supports for kinetic and structural analysis in the AFM. Large-scale domain formation caused by phase separation in the mixed systems does not occur on the Langmuir trough when the subphase is pure water (Maloney and Grainger, 1993). We have chosen to work with a Ca^{2+}-free subphase to avoid creating micron-sized domains characteristic of large-scale phase separation in the monolayers (Maloney and Grainger, 1993). Without calcium we were able to create a bilayer that resembles vesicular systems and that were more closely related to a bilayer that has been partially degraded by the enzyme (Nielsen et al., 1999).

Two layers were transferred onto the solid supports vertically at 1 mm/min, with a 15-min wait between the first and second layer. Only double layers with transfer ratios close to 1 were used (Fig. 1 *A*). Supported bilayers with an initial product concentration of 25%, 50%, 75%, and 100% were prepared. The supported bilayers were kept under water and immediately transferred to the fluid cell of the AFM.

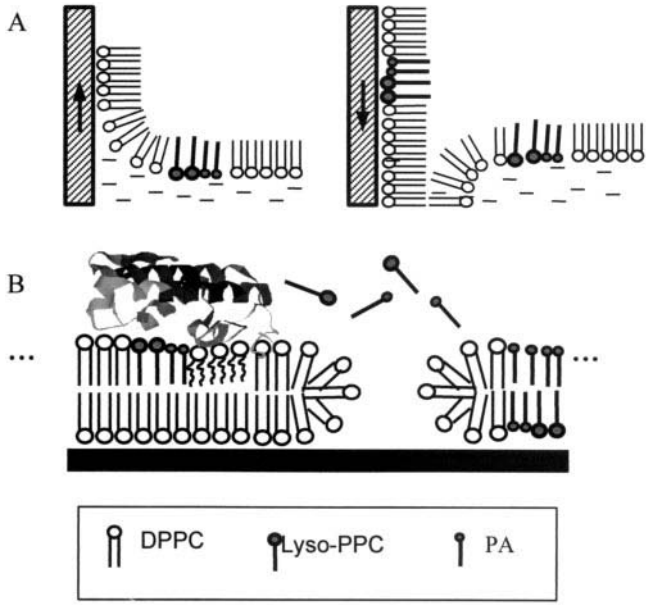

FIGURE 1 (*A*) Schematic illustration of the transfer of the mixed monolayers to a solid support. First a monolayer of DPPC and products were transferred to the solid support, and then a double layer was formed on the down stroke of the support. (*B*) In the AFM, the bilayer was hydrolyzed by phospholipase A_2 (shown as its crystal structure), which created additional product molecules. The structure of the bilayer was observed by the AFM. Especially the height difference between the top of the bilayer and the substrate and between the top and product regions can be seen in the images.

Enzyme and buffers

Snake venom PLA_2 from *Agkistrodon piscivorus piscivorus* (a gift from Prof. R. L. Biltonen, University of Virginia). We used a Hepes buffer (10 mM Hepes, 150 mM KCl, 30 μM $CaCl_2$, and 10 μM EDTA, pH 8.0), which prevents extensive calcium palmitate precipitation and minimizes changes in the Ca^{2+} concentration at the bilayer surface when the negatively charged fatty acid molecules are present. The enzyme concentration used was 10 nM.

Atomic force microscopy

A Nanoscope IIIa system (Digital Instruments, Santa Barbara, CA) equipped with a fluid cell was used for all imaging. A standard silicon O-ring was used to seal the fluid cell. The cell was flushed with Hepes buffer without enzyme before any imaging. Cantilevers with oxide-sharpened silicon nitride tips (NanoProbes, Santa Barbara, CA) with a nominal spring constant of 0.06 N/m was used for scanning. The bilayer was equilibrated in the fluid cell for at least 30 min to reduce cantilever drift before enzyme injection. All imaging was carried out in contact mode with a loading force of less than 500 pN, and the force was constantly kept at a minimum by manual adjustment of the set-point. The scan rate was 4 Hz (i.e., 2.1 min/image). To further minimize any influence of the tip on the hydrolysis, every other frame was scanned with the tip away from the surface except in the very beginning of the hydrolysis. Under these conditions, the bilayer can be imaged repeatedly (Shao and Yang, 1995; Shao et al., 1996), even during hydrolysis (Grandbois et al., 1998; Nielsen et al., 1999). As an additional control, the scan area was increased and/or moved after each experiment to check that hydrolysis had taken place over the entire sample and that these other areas appeared similar to the one

TABLE 1 Summary of the kinetic and structural data obtained from the hydrolysis experiments

Substrate (DPPC:products)	[PLA_2]	Initial defects observed in AFM	Lag time	v_{MAX}	Total hydrolysis
100:0 (Nielsen 1999)	84 nM	Structural	10–25 min	0.01–0.02 mmol DPPC/min/mol PLA_2	90–100%
75:25	10 nM	Structural	0 min	0.02–0.07 mmol	10–50%
50:50		Structural		DPPC/min/mol PLA_2	
25:75		Structural & compositional			
0:100		Structural			

analyzed. This was true for all the experiments dealt with in this report. All images have been plane fitted to remove sample tilt. Fig. 1 *B* schematically illustrates the situation in the fluid cell during the enzyme hydrolysis of the bilayer. Notice the distinct height difference between the top of the bilayer and bilayer deep holes and small depressions caused by phase separation in the bilayer, as these will show up on the AFM images.

Image analysis

The primary observable in the experiments is the amount of bilayer that is desorbed from the support, leaving bilayer deep defects behind. Once released from the bilayer the products are readily soluble in the buffer in the fluid cell of the AFM. The overall lipid concentration is ~2 μM, which is below the critical micellar concentration of the products (Marsh, 1990; Høyrup et al., 2001). A quantification of the defect areas was obtained through image analysis using NIH Image software (http://rsb.info.nih.gov/National Institutes of Health-image). Briefly, all images were subjected to a threshold filter followed by an automatic identification and area determination procedure that gives the area of individual holes in the bilayer. The sum of the area of the holes was used as an estimate for the degree of hydrolysis. The validity of using this estimate has been studied by Speijer et al. (1996). They found for a supported bilayer of radioactive labeled dioleoylphosphatidylcholine (DOPC) that less than 2% of the desorbed molecules were unhydrolyzed DOPC. This means that the hydrolysis products may go into solution, whereas the substrate will not dissolve and therefore will remain at the support.

RESULTS

We used AFM to characterize the structural appearance of supported lipid bilayers. Image analysis of the AFM images was used to quantify hole growth in the presence of PLA_2. The height differences present in the bilayers were a result of phase separation or incomplete coverage of the support. The latter appeared as holes in the bilayer. With the enzyme present holes in the bilayer grew and new ones were created. Hydrolysis of the phospholipid led to product formation. The product molecules did not remain in the bilayer but desorbed from the support, thus creating a hole in the bilayer. Determining the area fraction of holes in the membrane at a given time gave a measure of the degree of hydrolysis. Measured this way, the degree of hydrolysis was influenced by desorption of unhydrolyzed DPPC.

The structural appearance of the supported bilayers could be characterized as follows. The majority of the area between 95% and 100% of all freshly prepared bilayers transferred to the AFM consisted of a uniform flat bilayer with a composition given by the composition of the monolayer on the Langmuir trough. In addition to the uniform structure, two additional features were observed. The first was bilayer deep holes in the membrane where the mica was not covered with molecules. We shall refer to these defects as structural defects and use them as an indicator for the degree of hydrolysis. As indicated in Table 1, the structural defects were present on all samples before enzyme injection. The concentration of these defects varied between samples, and they were a result of the transfer process. However, for all samples, the area fraction covered by this type of defects was below 5%. The average depth of these defects was 6 nm, in good agreement with earlier measurements of the thickness of a DPPC bilayer in the gel phase made by others and ourselves (Shao et al., 1996; Grandbois et al., 1998; Nielsen et al., 1999). Individual defects had different shapes and sizes and covered areas of less than 0.6 μm^2.

A second type of defect was characterized as small depressions 3–5 Å in depth relative to the top of the uniform bilayer. In contrast to the structural defects the depressions arose because of lateral heterogeneity in the membrane caused by product domain formation as a result of phase separation. We shall hence refer to these defects as compositional defects. The lateral size of the defects also varied but was generally a factor of 10 smaller than for the structural defects where individual defects covered areas of less than 0.05 μm^2.

Compositional defects were observed just before the burst in pure DPPC bilayers (Nielsen et al., 1999) and for bilayers initially containing 75% products. Despite the high product concentration in the 25% and 50% samples, no signs of initial compositional defects were found (data not shown). With 75% products initially present, it was only a very small area fraction (~1%) of the bilayer that had the characteristics of the compositional defects. Fig. 2 *A* shows an AFM image of the initial appearance of a bilayer with 75% products. Arrows mark the two different defect types. When bilayers were composed of lyso-PPC and PA (1:1), a uniform flat bilayer containing only structural defects reappeared (data not shown). These bilayers were fragile, and the mechanical influence of the tip created an increasing area fraction of the defects. Product domains were found to be stable in the presence of DPPC where repeated scanning of the same area did not create additional defects.

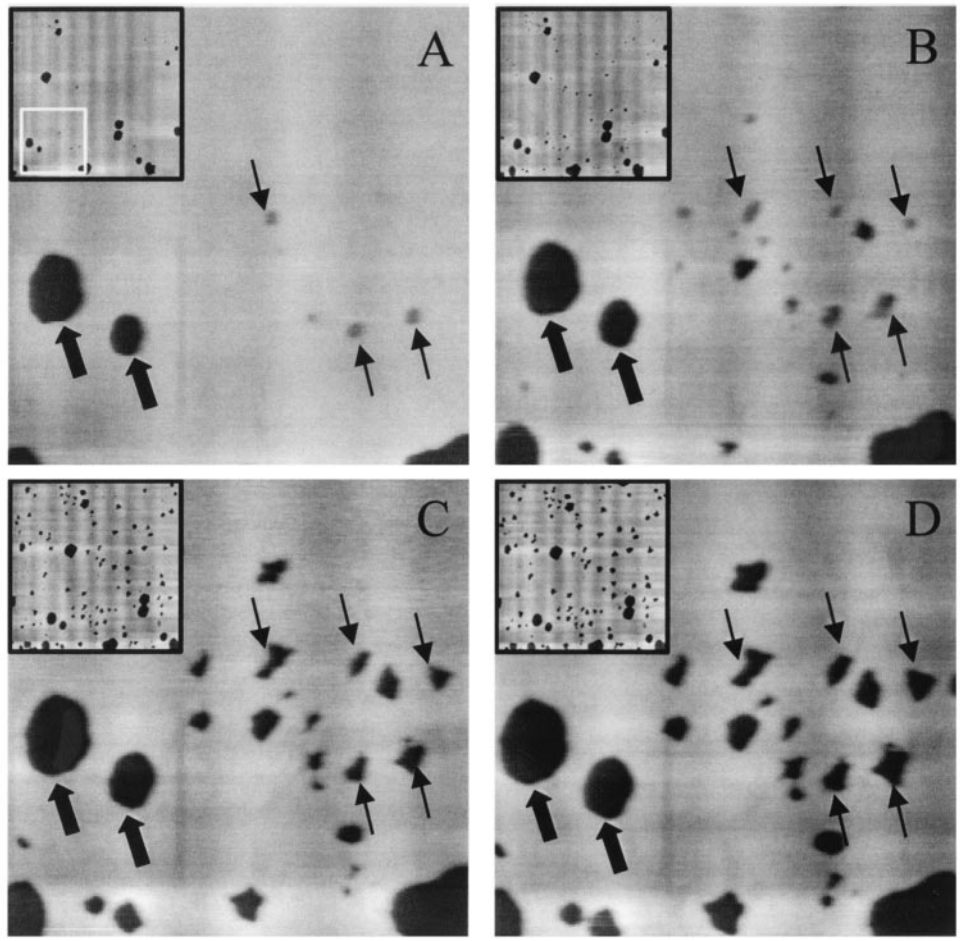

FIGURE 2 Images of a bilayer containing 75% product molecules subject to the hydrolysis by PLA_2. (*A–D*) The 5×5 μm^2 images were selected from a larger image of 15×15 μm^2 (shown in the *upper left corner* of each image). The white square in the 15×15 μm^2 image (*A*) shows were the enlarged region has been selected. Arrows mark the two different defect types discussed in the text. The block arrows point to structural defects and the thin arrows to compositional defects (see text for definitions of defect types). The arrows point to the same defects in each image. (*A*) Before the injection of the phospholipase; (*B*) At 2 min after PLA_2 addition, new structural defects were seen and also many new compositional defects; (*C*) At 4 min after PLA_2 addition, almost all compositional defects had turned into structural ones; (*D*) At 6 min after PLA_2 addition, all the structural defects then grew with time (see Fig. 3 for kinetic analysis).

Fig. 3 shows the reaction time course of the hydrolysis of a bilayer initially containing 75% products. The area of the structural defects had been quantified by image analysis and was used as an estimate of the degree of hydrolysis. The hydrolysis reaction started immediately after enzyme injection without any signs of a latency period and proceeded at maximum velocity until it eventually slowed down most likely because of the lack of substrate molecules. The reaction kinetics exhibited the same pattern for all bilayers initially containing products. Table 1 summarizes the results for bilayers with different initial product concentration. For comparison we have included the data from Nielsen et al. (1999) for pure DPPC bilayers with no products initially present. From the table it is clear that when products were initially present in the bilayer the hydrolysis started immediately after enzyme injection. We have compared the initial area growth rate, which is equal to the maximum area growth rate for the layers that initially contained products, with the maximum area growth rate obtained for the DPPC bilayers without initial products (Nielsen et al., 1999). When products were initially present, the initial area growth rate was slightly higher than the maximum area growth rate after the burst for the pure DPPC bilayers. The total hydrolyzed amount quantified as the area fraction of structural defects caused by dissolution of product molecules also changed from 90% to 100% for pure DPPC bilayers to between 10% and 50% for bilayers initially containing products.

The first frames from the complete image series analyzed in Fig. 3 are shown in Fig. 2, *A–D*. These images illustrate the temporal development of the action of PLA_2 on a bilayer that initially has both structural and compositional defects present (25% DPPC and 75% products). Upon the addition of PLA_2, it is evident that the number of structural defects increases with time as a sign of the hydrolysis process. More important, however, are the regions where the new structural defects appeared. New structural defects were generated in the regions of the bilayer with compositional defects that were attacked right away, and the molecules in these regions were solubilized in the buffer. The initial structural defects were also growing in size, but the rate of relative area increase was much slower than for the compositional defects, as illustrated in Fig. 4 *A*. The relative area increase was found by dividing the area difference between two consecutive frames with the initial area of the defect. This can be expressed as $\Delta A_{relative} = (A_{t2} - A_{t1})/A_{t0}$, where A_{t2}

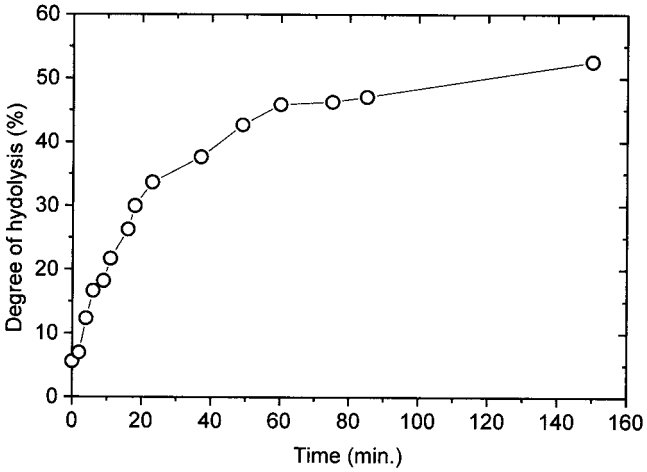

FIGURE 3 Kinetic analysis of the hydrolysis of a bilayer that initially contained 75% products. The degree of hydrolysis was determined from image analysis. The area fraction of structural defects equals the degree of hydrolysis. The hydrolysis began immediately after enzyme injection without any sign of a latency period.

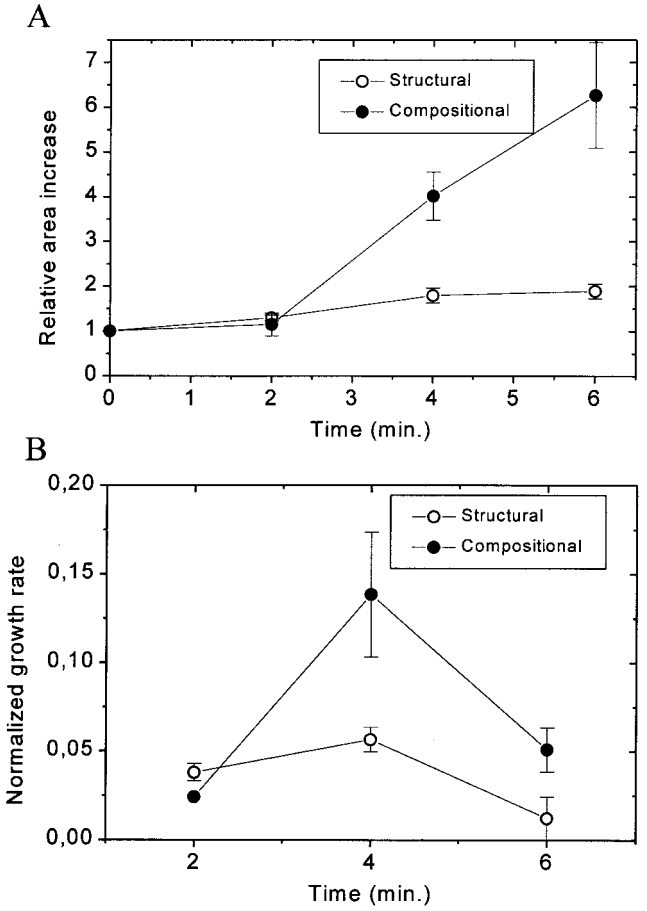

FIGURE 4 Comparison between the early time development of the structural and compositional defects. The defects chosen at time zero were identified on later frames such that they were the same defects that had been analyzed. Error bars represent 1 SD of the determination. (*A*) The relative area increase as a function of time. The area determined in each image was normalized by the area at time zero for each defect individually. (*B*) The normalized growth rate as a function of time. Here the area increase between two consecutive images was divided by the perimeter of the defect in the first image. This illustrates that the initial growth rate was larger for the compositional defects and that once the defects had become holes (i.e., like structural defects) their growth rate fell back to that of the structural defects.

and A_{t1} are the area of the defect at time t_2 and t_1 in two consecutive AFM images. A_{t0} is the initial area of the defects before addition of PLA_2. The rate of the relative area increase was 8.6 times larger for the regions where there was phase separation. We have previously showed that during the fast hydrolysis the area growth rate of the defects was proportional to the length of the edge around defect areas (Nielsen et al., 1999). If this were the case, it is trivial, when normalizing by the area, that small defects as the compositional ones will grow faster than the larger structural defects simply because of their larger perimeter-to-area ratio. Instead of normalizing by area, we normalized the area increase by the perimeter of the defects to illustrate any differences in the growth rate of the two defect types. This normalization scheme can be expressed as $\Delta A_{\text{normalized}} = (A_{t2} - A_{t1})/p_{t1}$, where A_{t2} and A_{t1} are the same as above and p_{t1} is the perimeter of the defect at time t_1. Fig. 4 *B* shows the results of this calculation. First, the growth rates of the compositional defects were larger than that of the structural defects. It was, however, during the initial attack on the compositional defects that their growth rate peaked. After they became holes and changed into new structural defects, their growth rates approached that of the other structural defects. The results in Fig. 4 *B* indicate that the enzyme had a preference for the compositional defects compared with the structural defects.

DISCUSSION

Our structural study aims to clarify how a high initial product concentration influences the hydrolysis of supported bilayers by PLA_2 as well as the lateral bilayer structure. We furthermore try to elucidate the relation between the nonequilibrium structure created during the initial course of the hydrolysis to the structure of the membrane with high product content where phase separation occurs. Phase separation has previously been reported once a critical mole fraction (~0.08) has been formed in vesicles (Apitz-Castro et al., 1982; Burack and Biltonen 1994; Burack et al., 1997a,b). The introduction of hydrolysis products into vesicles have the additional effect, besides the phase separation, that large morphological changes may take place and that these alone have a pronounced effect on the hydrolysis process (Callisen and Talmon, 1998). In monolayers, large-scale phase separation between lyso-PPC and PA has been observed as well as domain formation in the ternary system DPPC:lyso-PPC:PA (Maloney and

Grainger, 1993). These domains are negatively charged, which indicates that they mainly consist of PA molecules. PLA_2 has a preference for these fatty-acid-enriched domains and PLA_2 clusters underneath them (Grainger et al., 1989, 1990; Riechert et al., 1992). Any domain formation in monolayers, however, cannot be detected in the absence of calcium, independent of product concentration (Maloney and Grainger, 1993). The AFM images of the bilayers with 75% products, however, showed compositional defects indicative of some lateral phase separation. The domain size is fairly small, and these domains would be undetectable with fluorescence microscopy. The molecules constituting the compositional defects are likely to be highly enriched in PA. We base this interpretation on the previous results showing that during hydrolysis both product molecules are released from the membrane, but the lyso-lipid is released to a larger extent, resulting in a fatty-acid-rich region in the membrane (Tatulian, 2001). In addition, it is well established that PLA_2 has a preference for negatively charged bilayers or negatively charged regions of the bilayer caused by its net positive charge (Ghomashchi et al., 1991; Burack et al., 1995; Zhou and Schulten, 1996; Henshaw et al., 1998). This preference is illustrated in Fig. 2 where the addition of enzyme causes immediate desorption of the phase-separated regions. Finally, the loss of the PC headgroup makes the PA molecules shorter, which would make regions in the bilayer enriched in PA appear as small depressions in accordance with our observations. The length decrease of the molecule caused by the loss of the PC headgroup is comparable to the 3–5 Å that we measure. In our earlier work (Nielsen et al., 1999), compositional defects similar to the ones presented in Fig. 2 were observed. Such defects were not observed in the DPPC bilayer in the absence of PLA_2 but appeared only after enzyme addition. This corroborates our interpretation of the chemical composition of the compositional defects.

AFM has previously been used as a kinetic tool to study the hydrolysis of supported lipid bilayers by PLA_2 (Grandbois et al., 1998; Nielsen et al., 1999). The suitability of the AFM method to study enzyme kinetics depends on the experimental conditions. The temporal resolution is fairly low, on the order of 1 or 2 min (for the areas in question, generally scanning smaller areas would improve the temporal resolution). When choosing the area on the sample for which the simultaneous kinetic and structural data are to be collected, one faces the compromise between high lateral resolution, which would require an area as small as possible, and good kinetic statistics, which would require the imaging of an area as large as possible. We have chosen image sizes ranging from $5 \times 5\ \mu m^2$ to $15 \times 15\ \mu m^2$, which gives good kinetic data as illustrated in Fig. 2. The figure shows that the hydrolysis process is clearly taking place within the frame of view and that there are primary attack points that lead to new defect formation and defect growth. The lateral resolution ranges from 10 to 30 nm, which is enough to see small channels that are the result of the hydrolysis by a single enzyme (Grandbois et al., 1998; Nielsen et al., 1999). Despite the apparent shortcoming of AFM as a kinetic tool, the low enzyme concentration used in the experiments makes the reaction sufficiently slow, and we are able to follow the temporal evolution of the hydrolysis reaction. The kinetic analysis provides a good control that the experiments are carried out under identical conditions and that any influence from the scanning of the tip is minimized, as the maximum area growth rate and the total hydrolysis (Table 1) would change significantly between experiments if they were a result primarily of the scanning motion. The apparent increase in the maximum area growth rate when products are initially present can be rationalized in terms of our primary observable. A bilayer containing products is more susceptible to attack by the enzyme (Burack et al., 1993; Henshaw et al., 1998), which in turn leads to desorption of not only newly hydrolyzed lipids but also some of the product molecules already present in the bilayer. Structural defects emerge and the degree of hydrolysis is biased by the desorption of lyso-PPC and PA initially present in the bilayer. Addition of the enzyme thus has a strong perturbing effect on the bilayer. Product molecules that were originally situated within the bilayer and were stable during scanning suddenly leave the bilayer upon the addition of PLA_2 (discussed below).

The extent of the hydrolysis at the end of the experiments was not, surprisingly, significantly lower for the ternary systems. Again, our estimate of the total hydrolysis is based entirely on the area fraction of the structural defects. Any hydrolysis that does not result in hole growth or creation of new holes will not be included in the measurement. The significance of our results is therefore contained in the high-resolution structural data for which the AFM is an excellent tool.

Any defects in a phospholipid bilayer will promote the degradation of the bilayer by PLA_2, whether the defects are of compositional origin or they are a result of fluctuations or they are holes in the bilayer. The presence of defects and especially products leads to a decrease in the latency period, which is equivalent to an increase in the susceptibility of the bilayer to hydrolysis. As shown in Fig. 2 *A*, we observe two distinct types of defects present in the initial substrate. Both defect types have been shown to serve as sites for the enzymatic attack (Grandbois et al., 1998; Nielsen et al., 1999). The structural defects are primary attack points probably caused by looser packing of lipids around the edge (Grandbois et al., 1998). The compositional defects composed of products promote the recruitment of phospholipase molecules at the surface because of their affinity toward negatively charged fatty acid molecules. This also results in faster break-up of the bilayer because of the elimination of the latency phase. When both defect types are present simultaneously they are both primary attack points for the enzyme, as the area of both types increases with time. The

normalized growth rate (Fig. 4 *B*) is, however, much greater for the compositional defects in the beginning of hydrolysis, illustrating that this type of defect is a more effective promoter of the increased susceptibility. With time, the compositional defects become holes and turn into structural defects, and their growth rate approaches the rate of the other structural defects. This further underlines the ability of these phase-separated regions to recruit or activate PLA_2 molecules. Therefore, these regions play a more important role in the promotion of the hydrolysis than the structural defects. The ability to compare two different defect types and the quantitative analysis of the time development of individual defects are unique features of our experiments.

The presence of products even in very high concentrations is on its own not enough to destroy the structural integrity of the supported bilayers. A similar statement is valid for vesicles where structural integrity can be attained even after the addition of large mole fractions of products up to 0.4 achieved by co-sonication of the phospholipid and the product molecules (Bhamidipati and Hamilton, 1995). This is in contrast to the situation with vesicles when the enzyme present. Here large-scale morphological changes and loss of structural integrity is observed at very low degrees of hydrolysis (5–10%) during the latency period (Callisen and Talmon, 1998). Phase-separated product domains are also stable in the AFM experiments as long as the enzyme has not been added. Once present, however, the bilayer immediately begins to lose its structural integrity. We rule out that the injection of PLA_2 and the flow caused thereby destabilizes the product domains because in the initial preparation the cell is flushed with buffer causing a similar flow. The compositional defects observed are thus stable during gentle flushing of the cell. The bilayer is strongly perturbed by the presence of PLA_2, which in combination with the hydrolysis products rips the membrane apart. The generation of new defects and the growth of existing ones are thus the result of the combined action of the generated product domains and the bilayer-perturbing effect of the enzyme as it scoots (Jain et al., 1994) over the bilayer surface. The bilayer-perturbing effect of the phospholipase could in the current context be investigated in greater detail by addition of an inactive PLA_2 to see whether this would lead to desorption of product-rich domains. A clarification must, however, await future experiments.

The absence of a lag time and compositional defects for 25% and 50% products suggests a mechanism for activation of PLA_2 by the products, which is independent of the presence of compositional defects. This raises a question about length scales. How large do a product domain have to be to activate PLA_2? And how large does it have to be to be observed in the AFM when kinetic data has to be acquired simultaneously? We cannot, based on our experimental approach, rule out the presence of short lag times for the cases of 25% and 50% products. Similarly, if a compositional defect has to consist of only a small number of molecules before PLA_2 can sense it, then it would be undetectable by AFM. New compositional defects are, however, created during the hydrolysis, which puts emphasis on the length scale argument. Areas enriched in products exist that are too small to be detected. After a short time in the presence of PLA_2, these areas become compositional defects as seen in Fig. 2 *B*. The activation of PLA_2 is therefore not exclusively dependent on the presence of compositional defects of the sizes shown in Fig. 2. The activation by the product molecules, whether present as compositional defects or not, may, however, be the same. The advantage of the compositional defects is that we are able to follow their evolution in time, which clearly illustrates the preference of PLA_2 for these defects in comparison with the structural ones. In relation to the structural development during the latency period, we are able to compare directly with our earlier results (Nielsen et al., 1999). We have argued that the compositional defects are a result of phase separation at high product concentrations and that these defects must be enriched in PA. The similarity between these preformed defects and those observed toward the end of the latency phase (Nielsen et al., 1999) is striking. Their depths are identical, which support the interpretation that the domains created by the enzyme close to the burst are of the same composition as the compositional defects. The domains created by PLA_2 do not reflect the equilibrium structure of the bilayer, which is especially true for a bilayer in the gel phase, whereas the compositional defects created on the Langmuir trough, is closer to equilibrium. Nevertheless, product domains have a pronounced effect on the susceptibility of the bilayer to the attack by PLA_2 observed as a burst in the hydrolysis for the pure DPPC bilayers (Nielsen et al., 1999) and as a high growth rate in the systems containing products as shown in the present paper.

In summary, we have investigated the hydrolysis of supported product containing bilayers by PLA_2 using AFM. As expected, a latency period was not observed for the product concentrations in question. Bilayers that initially contained 75% products show two distinct types of defects, structural and compositional. Using image analysis, we have been able to quantify the relative growth rates of these defect types. The results show an initial preference for the compositional defects over the structural ones. Domain formation during the slow hydrolysis in the latency period (Nielsen et al., 1999) shows remarkable similarity to the compositional defects shown in the present report. This result supports the hypothesis that products are important determinants of bilayer susceptibility and consequently PLA_2 activity.

We thank P. Høyrup, O. G. Mouritsen, and Allan Svendsen for stimulating discussion.

This work was supported by the Danish Research Council, the Danish Technical Research Council, Novo Nordisk A/S, and EU the Biotechnology program Lipid Structure and Lipases.

REFERENCES

Apitz-Castro, R., M. K. Jain, and G. H. De Haas. 1982. Origin of the latency phase during the action of phospholipase A2 on unmodified phosphatidylcholine vesicles. *Biochim. Biophys. Acta.* 688:349–356.

Balashev, K., T. R. Jensen, K. Kjaer, and T. Bjørnholm. 2001. Novel methods for studying lipids and lipases and their mutual interaction at interfaces. I. Atomic force microscopy. *Biochimie.* 83:387–397.

Beisson, F., A. Tiss, C. Rivière, and R. Verger. 2000. Methods for lipase detection and assay: a critical review. *Eur. J. Lipid Sci. Technol.* 102: 133–153.

Bhamidipati, S. P., and J. A. Hamilton. 1995. Interactions of lyso 1-palmitoylphosphatidylcholine with phospholipids: a C-13 and P-31 NMR study. *Biochemistry.* 34:5666–5677.

Brown, S. D., B. L. Baker, and J. D. Bell. 1993. Quantification of the interaction of lysolecithin with phosphatidylcholine vesicles using bovine serum-albumin: relevance to the activation of phospholipase-A2. *Biochim. Biophys. Acta.* 1168:13–22.

Burack, W. R., and R. L. Biltonen. 1994. Lipid bilayer heterogeneities and modulation of phospholipase A2 activity. *Chem. Phys. Lipids.* 73: 209–222.

Burack, W. R., A. R. G. Dibble, M. M. Allietta, and R. L. Biltonen. 1997b. Changes in vesicle morphology induced by lateral phase separation modulate phospholipase A2 activity. *Biochemistry.* 36:10551–10557.

Burack, W. R., A. R. G. Dibble, and R. L. Biltonen. 1997a. The relationship between compositional phase separation and vesicle morphology: implications for the regulation of phospholipase A2 by membrane structure. *Chem. Phys. Lipids.* 90:87–95.

Burack, W. R., M. E. Gadd, and R. L. Biltonen. 1995. Modulation of phospholipase A2: identification of an inactive membrane-bound state. *Biochemistry.* 34:14819–14828.

Burack, W. R., Q. Yuan, and R. L. Biltonen. 1993. Role of lateral phase-separation in the modulation of phospholipase-A2 activity. *Biochemistry.* 32:583–589.

Callisen, T. H., and Y. Talmon. 1998. Direct imaging by cryo-TEM shows membrane break-up by phospholipase A2 enzymatic activity. *Biochemistry.* 37:10987–10993.

Fernández, M. S., R. Mejia, and E. Zavala. 1991. The interfacial calcium ion concentration as modulator of the latency phase in the hydrolysis of dimyristoylphosphatidylcholine liposomes by phospholipase A2. *Biochem. Cell Biol.* 69:722–727.

Ghomashchi, F., B-Z. Yu, O. Berg, J. M. Jain, and M. H. Gelb. 1991. Interfacial catalysis by phospholipase-A2: substrate specificity in vesicles. *Biochemistry.* 30:7318–7329.

Grainger, D. W., A. Reichert, H. Ringsdorf, and C. Salesse. 1989. An enzyme caught in action: direct imaging of hydrolytic function of phospholipase A2 in phosphatidylcholine monolayers. *FEBS Lett.* 252: 73–82.

Grainger, D. W., A. Reichert, H. Ringsdorf, and C. Salesse. 1990. Hydrolytic action of phospholipase-A2 in monolayers in the phase-transition region: direct observation of enzyme domain formation using fluorescence microscopy. *Biochim. Biophys. Acta.* 1023:365–379.

Grandbois, M., H. Clausen-Schaumann, and H. Gaub. 1998. Atomic force microscope imaging of phospholipid bilayer degradation by phospholipase A2. *Biophys. J.* 74:2398–2404.

Henshaw, J. B., C. A. Olsen, A. R. Farnbach, K. H. Nielson, and J. D. Bell. 1998. Definition of the specific roles of lysolecithin and palmitic acid in altering the susceptibility of dipalmitoylphosphatidylcholine bilayers to phospholipase A(2). *Biochemistry.* 37:10709–10721.

Hønger, T., K. Jørgensen, R. L. Biltonen, and O. G. Mouritsen. 1996. Systematic relationship between phospholipase A2 activity and dynamic lipid bilayer microheterogeneity. *Biochemistry.* 35:9003–9006.

Hønger, T., K. Jørgensen, D. Stokes, R. L. Biltonen, and O. G. Mouritsen. 1997. Phospolipase A2 activity and physical properties of lipid-bilayer substrates. *Methods Enzymol.* 286:168–190.

Høyrup, P., J. Davidsen, and K. Jørgensen. 2001. Lipid membrane partitioning of lysolipid and fatty acids: effects of membrane phase. *J. Phys. Chem. B.* 105:2649–2657.

Jain, M. K., C. D. Krause, J. T. Buckley, T. Bayburt, and M. H. Gelb. 1994. Characterization of interfacial catalysis by *Aeromonas hydrophila* lipase/acyltransferase in the highly processive scooting mode. *Biochemistry.* 33:5011–5020.

Jensen, T. R., K. Balashev, T. Bjørnholm, and K. Kjaer. 2001. Novel methods for studying lipids and lipases and their mutual interaction at interfaces. II. Surface sensitive synchrotron x-ray scattering. *Biochimie.* 83:399–408.

Kudo, I., M. Murakami, S. Hara, and K. Inoue. 1993. Mammalian nonpancreatic phospholipases A2. *Biochim. Biophys. Acta.* 117:217–231.

Maloney, K. M., and D. W. Grainger. 1993. Phase separated anionic domains in ternary mixed lipid monolayers at the air-water interface. *Chem. Phys. Lipids.* 65:31–42.

Marsh, D. 1990. Handbook of Lipid Bilayers. CRC Press, Boca Raton, FL.

Mayer, R. J., and L. A. Marshall. 1993. New insights on mammalian phospholipase-A2(s): comparison of arachidonoyl-selective and arachidonoyl-nonselective enzymes. *FASEB J.* 7:339–348.

Muderhwa, J. M., and H. L. Brockman. 1992. Lateral lipid distribution is a major regulator of lipase activity: implications for lipid-mediated signal transduction. *J. Biol. Chem.* 267:24184–24192.

Nielsen, L. K., T. Bjørnholm, and O. G. Mouritsen. 2000. Fluctuations caught in the act. *Nature.* 404:352.

Nielsen, L. K., J. Risbo, T. H. Callisen, and T. Bjørnholm. 1999. Lag-burst kinetics in phospholipase A2 hydrolysis of DPPC bilayers visualized by atomic force microscopy. *Biochem. Biophys. Acta.* 1420:266–271.

Riechert, A., H. Ringsdorf, and A. Wagenknecht. 1992. Spontaneous domain formation of phospholipase A2 at interfaces: fluorescence microscopy of the interaction of phospholipase A2 with mixed monolayers of lecithin, lysolecithin and fatty acid. *Biochim. Biophys. Acta.* 1106: 178–188.

Shao, Z., J. Mou, D. M. Czajkowsky, J. Yang, and J.-Y. Yuan. 1996. Biological atomic force microscopy: what is achieved and what is needed. *Adv. Phys.* 45:1–86.

Shao, Z., and J. Yang. 1995. Progress in high resolution atomic force microscopy in biology. *Q. Rev. Biophys.* 28:195–251.

Speijer, H., P. L. A. Giesen, R. F. A. Zwaal, C. E. Hack, and W. T. Hermens. 1996. Critical micelle concentrations and stirring are rate limiting in the loss of lipid mass during membrane degradation by phospholipase A2. *Biophys. J.* 70:2239–2247.

Tatulian, S. A. 2001. Toward understanding interfacial activation of secretory phospholipase A2 (PLA2): membrane surface properties and membrane-induced structural changes in the enzyme contribute synergistically to PLA2 activation. *Biophys. J.* 80:789–800.

Vadas, P., J. Browning, J. Edelson, and W. Pruzanski. 1993. Extracellular phospholipase-A2 expression and inflammation: the relationship with associated disease states. *J. Lipid Mediat.* 8:1–30.

Waite, M. 1991. Phospholipases. *In* Biochemistry of Lipids, Lipoproteins and Membranes. D. E. Vance and J. Vance, editors. Elsevier, Amsterdam. 269–295.

Wilson, H. A., J. B. Waldrip, K. H. Nielson, A. M. Judd, S. K. Han, W. Cho, P. J. Sims, and J. D. Bell. 1999. Mechanisms by which elevated intracellular calcium induces S49 cell membranes to become susceptible to the action of secretory phospholipase A2. *J. Biol. Chem.* 274: 11494–11504.

Zhou, F., and K. Schulten. 1996. Molecular dynamics study of phospholipase A2 on a membrane surface. *Proteins.* 25:12–27.